CHEMISTRY
A EUROPEAN JOURNAL

DOI: 10.1002/chem.200600126

# Triply Fused $Zn^{II}$–Porphyrin Oligomers: Synthesis, Properties, and Supramolecular Interactions with Single-Walled Carbon Nanotubes (SWNTs)

**Fuyong Cheng,[a] Sheng Zhang,[b] Alex Adronov,*[a] Luis Echegoyen,*[b] and François Diederich*[c]**

**Abstract:** The photophysical, electrochemical, and self-assembly properties of a novel triply fused $Zn^{II}$–porphyrin trimer were investigated and compared to the properties of a triply fused porphyrin dimer and the analogous monomer. The trimer exhibited significantly red-shifted absorption bands relative to the corresponding monomer and dimer. Electrochemical investigations indicated a clear trend in redox properties amongst the three porphyrin structures, with the lowest oxidation potential and the lowest HOMO–LUMO gap exhibited by the triply fused trimer. This electrochemical behavior is attributed to the extensive π-electron delocalization in the trimeric structure relative to the monomer and dimer. Additionally, it was found that the trimer forms extremely strong and nearly irreversible supramolecular interactions with single-walled carbon nanotubes (SWNTs), resulting in stable solutions of porphyrin–nanotube complexes in THF. Formation of these complexes required the addition of trifluoroacetic acid (TFA) to the solvent. This allowed the oligomers to make close contact with the nanotubes, enabling the formation of stable supramolecular assemblies. Atomic force microscopy (AFM) was used to observe the supramolecular porphyrin–nanotube complexes and revealed that the porphyrin trimer formed a uniform coating on the SWNTs. Height profiles indicated that nanotube bundles could be exfoliated into either individual tubes or very small bundles by exposure to the porphyrin trimer during sonication.

**Keywords:** electrochemistry · nanotubes · porphyrinoids · scanning probe microscopy · supramolecular chemistry

## Introduction

The fascinating properties of triply fused conjugated porphyrin oligomers originate from their completely planar structure and extended π-electron delocalization.[1,2] Relative to their singly bonded analogues, the absorption spectra of these flat, sheetlike molecules exhibit a remarkable red-shift of the lowest energy electronic transition, which progressively increases with increasing number of linked porphyrin units. A highly efficient synthetic methodology utilizing 2,3-dichloro-5,6-dicyano-*p*-benzoquinone (DDQ) and $Sc(OTf)_3$ to prepare triply fused pophyrins from singly, biaryl-type fused precursors was recently developed by Osuka and co-workers, and has been successfully applied to the synthesis of longer oligomers, up to the dodecamer.[3] These rigid, planar molecular tapes exhibit unusually low HOMO–LUMO gaps and one-electron oxidation potentials, and may eventually serve as molecular wires within electronic devices.[3] Recently, triply fused porphyrin dimers have been covalently derivatized with two $C_{60}$ molecules, resulting in a dyad structure capable of undergoing up to fifteen reversible electron transfer steps.[4] Moreover, photophysical investigations demonstrated that the dyad does not exhibit the classical behaviour documented for numerous porphyrin–fullerene dyads. Photoexcitation of the fullerene units resulted in

[a] Dr. F. Cheng, Prof. Dr. A. Adronov
Department of Chemistry, McMaster University
Hamilton, Ontario L8S 4M1 (Canada)
Fax: (+1) 905-521-2773
E-mail: adronov@mcmaster.ca

[b] Dr. S. Zhang, Prof. Dr. L. Echegoyen
Department of Chemistry
Clemson University, SC 29634 Clemson (USA)
Fax: (+1) 864-656-6613
E-mail: luis@clemson.edu

[c] Prof. Dr. F. Diederich
Laboratorium für Organische Chemie, ETH-Hönggerberg
HCI, 8093 Zürich (Switzerland)
Fax: (+41) 1-632-1109
E-mail: diederich@org.chem.ethz.ch

Supporting information for this article is available on the WWW under http://www.chemistry.org or from the author.

quantitative sensitization of the weakly emitting lowest singlet level of the porphyrin dimer, while the fullerene emission was quenched. Additionally, supramolecular interactions between triply fused dimers and fullerenes have been investigated on a metal surface.[5] Self-assembly of fullerenes and porphyrins, governed by weak interactions between the two components, has led to unprecedented nanopatterned surfaces, as observed by scanning-tunnelling microscopy (STM).

Single-walled carbon nanotubes (SWNTs) also represent a class of fascinating molecules with extended π-electron delocalization. Through the seminal work of Dai,[6] Chen,[7] and Nakashima and co-workers,[8] it has become clear that the electron-deficient surface of SWNTs facilitates the binding of large electron-rich organic molecules through noncovalent π-stacking interactions. The mechanical strength and electrical conductivity of these materials impart significant potential as components of electronic nanodevices. Therefore, the coupling of SWNTs to other functional molecules has attracted significant attention. Several recent studies have shown that porphyrin molecules have a strong affinity for noncovalent adsorption to the SWNT surface.[8–14] This supramolecular SWNT–porphyrin interaction was shown to be selective for semiconducting rather than metallic SWNTs, allowing for the separation of nanotubes according to their conductivity properties.[9] In addition, the assembly of protonated porphyrins on the SWNT surface, followed by aggregation of large nanotube–porphyrin assemblies, has been reported.[12] Recently, we demonstrated that a conjugated porphyrin polymer, with the individual macrocycles linked by their *anti-meso* positions through buta-1,3-diynediyl moieties, exhibits a significantly stronger supramolecular interaction with SWNTs than monomeric porphyrins, allowing for effective solubilization of SWNTs and the formation of very stable solutions.[15] More interestingly, it was shown that SWNTs can act as a template to induce the neighboring porphyrin units of the conjugated porphyrin polymer to assume a coplanar orientation, resulting in increased π conjugation and a large red-shift (127 nm) of the Q-band absorption.

Although it was demonstrated that conjugated porphyrin polymers can strongly interact with SWNTs, the ability of each porphyrin monomer unit to rotate about the diacetylene linker limited the binding strength and allowed equilibration between bound and unbound polymers.[15] Triply fused $Zn^{II}$–porphyrin oligomers effectively restrict each repeat unit to a fully coplanar orientation, resulting in enhanced conjugation and electron-donating ability relative to all other porphyrin oligomers and polymers. These triply fused oligomers were therefore deemed ideal candidates for strong supramolecular interactions with SWNTs. In the present work, we demonstrate that these interactions do indeed occur and can lead to very strong, nearly irreversible binding of triply fused oligomers to the SWNT sidewall. Comparison of the triply fused dimer and trimer molecules, relative to the analogous monomeric control compound, uncovered clear trends not only in the interaction strength with SWNTs, but also in their spectroscopic and electrochemical properties.

## Results and Discussion

**Synthesis and characterization**: The structures of the triply fused dimer **2** and trimer **3**, and the control compound, monomer **1**, are depicted in Scheme 1. This series of rigid $Zn^{II}$–porphyrin oligomers have 3,5-di-*tert*-butylphenyl groups as *meso*-substituents to improve their solubility. At both ends of each compound, 4-cyanophenyl groups were introduced to enhance product polarity and therefore facilitate chromatographic separation of the intermediates and final products. These polar groups are also important for the formation of ordered, self-assembled porphyrin monolayers on surfaces.[5] As shown in Scheme 1, porphyrin **4**[12,16] was treated with two equivalents of *N*-bromosuccinimide (NBS), yielding dibromide **5**, which was treated with phenylboronic ester **6** by Pd-catalyzed Suzuki cross-coupling to give the bis(cyanophenyl)porphyrin derivative **1** in high yield. When porphyrin **4** was treated with one equivalent of NBS, followed by Suzuki cross-coupling with **6**, the (cyanophenyl)-porphyrin **8** was produced. Monomer **8** was converted into the triply fused dimer **2** in one step using the oxidative ring closure mediated by DDQ and $Sc(OTf)_3$, developed by Osuka and co-workers.[17]

The synthesis and chemical functionalization of triply fused porphyrin trimers has been practically unexplored outside of Osuka's original work, despite their extremely interesting structural and electronic properties.[2] We obtained the new cyano-functionalized triply fused porphyrin trimer **3**, by first preparing the *meso–meso*-linked trimer **11** by means of Pd-catalyzed cross-coupling. Porphyrin **8** was treated with NBS to yield bromoporphyrin **9**, followed by subsequent coupling with pinacolborane to give the porphyrin boronate ester **10** in 84% yield (Scheme 1). Cross-coupling of two equivalents of **10** with dibromoporphyrin **5** was carried out in a mixture of toluene and DMF in the presence of $Cs_2CO_3$ and a catalytic amount of $[Pd(PPh_3)_4]$, to give the targeted porphyrin trimer **11** in 17% yield. Four other side products were obtained, including the debrominated monomer **4**, the deboronated monomer **8**, the cross-coupled dimer **12**, and the homo-coupled dimer **13**. Separation of this product mixture was achieved by chromatography; flash chromatography on silica gel allowed isolation of **4**, **8**, and **12**, while a mixture of **11** and **13** was found to co-elute due to the relatively small polarity difference between the two compounds. However, preparative size-exclusion chromatography allowed for successful separation of **11** and **13**, because of the difference in their hydrodynamic volume. Trimer **11** was then efficiently oxidized by using DDQ and $Sc(OTf)_3$ to produce the desired triply fused trimer **3** in quantitative yield. The MALDI-TOF mass spectrum of **3** provided the most reliable evidence of its formation as it exhibited the expected molecular ion peak at 2435.0001 $g\,mol^{-1}$ ($[M]^+$, $C_{158}H_{150}N_{14}Zn_3$, calcd 2435.0037).

  

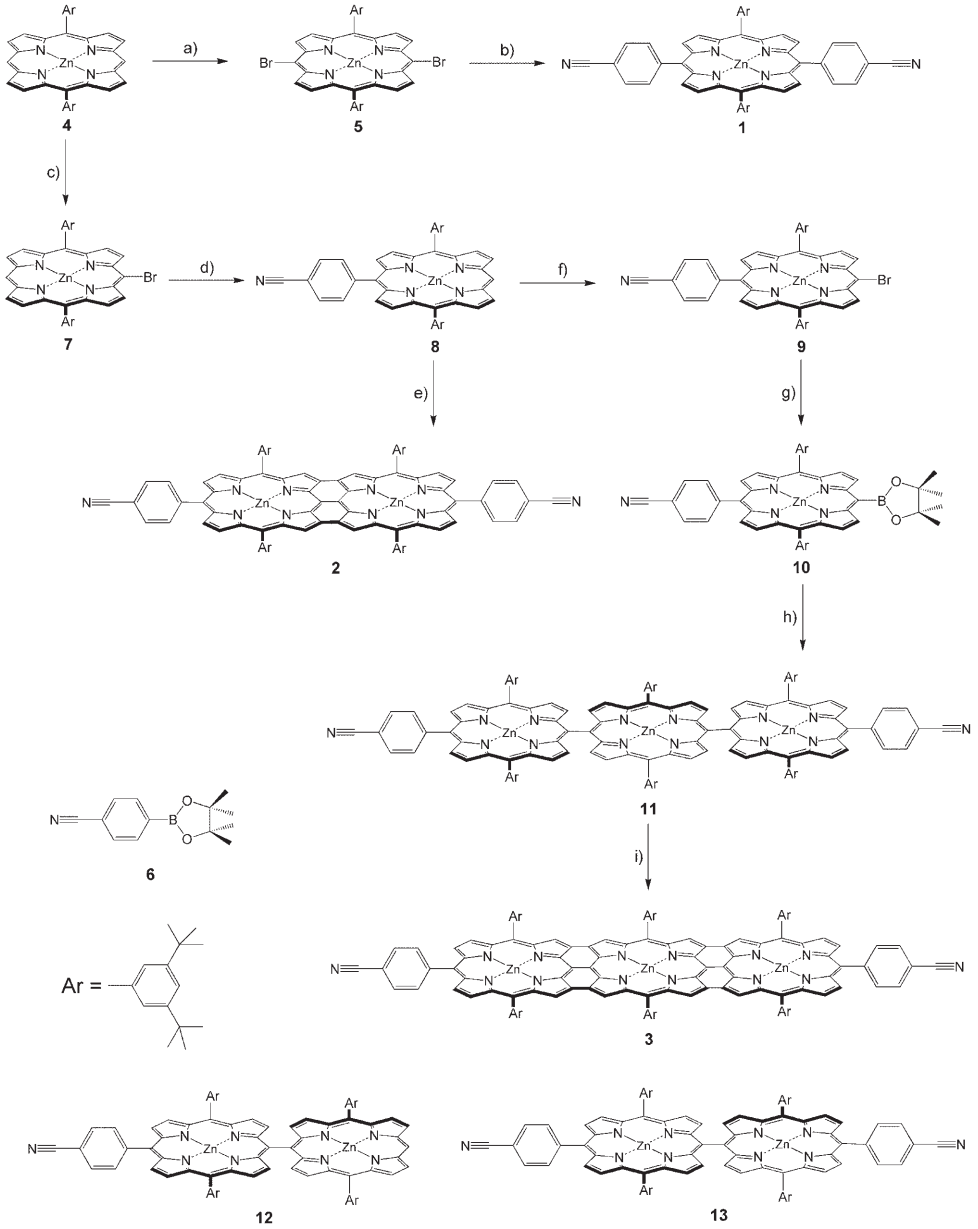


Scheme 1. a) NBS, $CH_2Cl_2$/pyridine, 0 °C, 10 min, 90 %; b) **6**, [$Pd(Ph_3P)_4$], $Cs_2CO_3$, toluene, Δ, 18 h, 97 %; c) NBS, $CH_2Cl_2$/pyridine, 0 °C, 10 min; d) **6**, [$Pd(Ph_3P)_4$] $Cs_2CO_3$, toluene, Δ, 18 h, 87 % over two steps; e) $Sc(OTf)_3$, DDQ, toluene, Δ, 2 h, 70 %; f) NBS, $CH_2Cl_2$/pyridine, 0 °C, 10 min, 86 %; g) pinacolborane, $Et_3N$, [$Pd(Ph_3P)_4$], $Cl(CH_2)_2Cl$, Δ, 1.5 h, 84 %; h) **5**, [$Pd(Ph_3P)_4$], $Cs_2CO_3$, toluene/DMF, 90 °C, 18 h, 17 %; i) $Sc(OTf)_3$, DDQ, toluene, Δ, 2 h, 100 %. NBS = *N*-bromosuccinimide; DDQ = 2,3-dichloro-5,6-dicyano-*p*- benzoquinone.

The $^1$H NMR spectrum of **3** ($CDCl_3/CS_2$) was consistent with the triply fused trimeric structure, but exhibited broadened signals, likely due to aggregation of these flat, symmetrical molecules in $CDCl_3$. Additionally, the byproduct **12** served as a building block for the synthesis of a triply fused porphyrin tetramer. By using $AgPF_6$ as the oxidant, dimer **12** was successfully converted into a *meso–meso*-linked porphyrin tetramer in 90 % yield and subsequently subjected to oxidative coupling (DDQ and $Sc(OTf)_3$) to produce the triply fused tetramer. Unfortunately, due to extremely poor solubility, isolation and characterization of this compound was not possible.

All three molecules of interest, monomeric **1**, dimeric **2**, and trimeric **3** displayed good solubility in organic solvents, such as $CH_2Cl_2$, $CHCl_3$, and THF. The solutions of the three compounds dramatically differed in color, with **1** forming a red solution, **2** a purple-blue solution, and **3** a green solution. Figure 1 shows the UV/Vis/NIR absorption spectra of the three compounds in $CHCl_3$. Clearly, a significant Q-band red-shift and intensity enhancement can be directly correlated to the extended π-electron delocalization that results from increasing the length of the triply fused oligomers. Thus, increasing the oligomeric length from dimeric **2** to trimeric **3** results in an extremely large red-shift of the Q-band

  

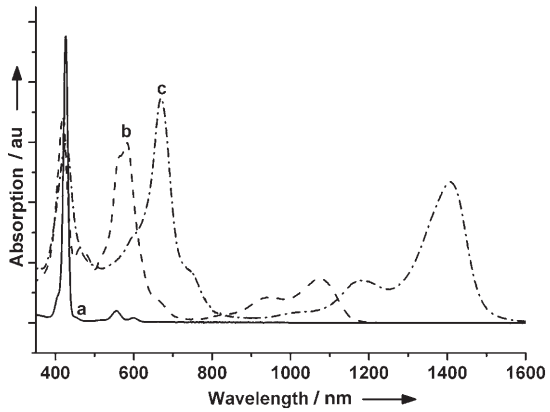


Figure 1. Electronic absorption spectra of a) monomeric **1**, b) dimeric **2**, and c) trimeric **3** porphyrins in $CHCl_3$.

absorption, amounting to 324 nm (3.83 eV). Additionally, in both the dimeric and trimeric systems, the Soret band exhibits splitting that is consistent with a previous report on related oligomers.[3]

**Electrochemical properties**: We have recently reported systematic studies of the electrochemical properties for a triply fused porphyrin dimer in comparison to monomeric analogues.[16] Here, we compare the redox properties of compounds **1**, **2**, and **3** as measured by cyclic (CV) and differential pulse voltammetry (DPV; Figures 2 and 3, respectively).

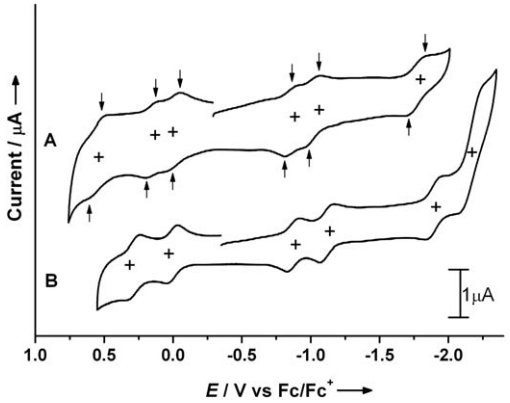


Figure 2. CVs of triply fused $Zn^{II}$–porphyrin trimer **3** in A) $CH_2Cl_2$ and B) THF at room temperature (+0.1 M $nBu_4NPF_6$).

The cyclic voltammogram of the triply fused Zn–porphyrin trimer **3** in $CH_2Cl_2$ is shown in Figure 2A. Six reversible redox couples were observed, with identical current for each of the peaks. Three reduction couples at −0.86, −1.01, and −1.77 V versus $Fc/Fc^+$ (ferrocene/ferricinium couple) correspond to the one-electron reductions of **3**, while three oxidation couples at 0.01, 0.16, and 0.55 V are due to its one-electron oxidations. The CV of **3** was also performed in THF (Figure 2B), and six reversible redox waves were again observed. Four equivalent reduction couples at −0.88, −1.12, −1.90, and −2.17 V versus $Fc/Fc^+$ correspond to four one-electron reductions of the compound, while two equivalent oxidation couples at 0.02 and 0.28 V are due to its one-electron oxidations. Compared to the CV in $CH_2Cl_2$, the CV in THF exhibits a larger separation of the first two reduction and oxidation reactions, which could be due to decreased aggregation of **3** in THF as a result of the coordinating ability of the furan oxygen atom to the $Zn^{II}$ center within each porphyrin repeat unit.[16] The lack of this interaction with $CH_2Cl_2$ potentially enables trimer aggregation, which decreases the barrier to oxidation and/or reduction of the molecules. The electrochemical gap (HOMO–LUMO gap) between the first oxidation and reduction potential of **3** is 0.87 V in $CH_2Cl_2$, and 0.90 V in THF.

Figure 3 compares the differential pulse voltammetry (DPV) data of the monomer, dimer, and trimer in THF. Clearly, the HOMO–LUMO gap of the trimer (1.00 V) is

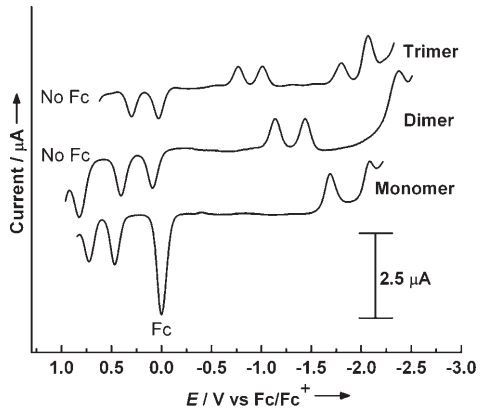


Figure 3. DPVs of monomeric **1**, dimeric **2**, and trimeric **3** in THF. Ferrocene (Fc) was added to the monomer solution as an internal standard.

significantly smaller when compared to those of the monomer (2.16 V) and the triply fused dimer (1.22 V). The first one-electron oxidation potential of the trimer (0.03 V) is also lower than those of the monomer (0.47 V) and the dimer (0.09 V). The significant difference in the voltammetric behavior of the three structures can be attributed to the increase in π-conjugation upon changing from the monomeric, to the dimeric, and to the trimeric porphyrin sheet.

**Supramolecular interactions with SWNTs**: The observed electrochemical properties of the triply fused dimer and trimer, especially their electron-donating character, encouraged us to investigate supramolecular interactions between these oligomers and SWNTs, which are known to be good electron acceptors.[18–22] In all of these studies, pristine SWNTs prepared by the HiPco process (Carbon Nanotechnologies, Houston, TX) were used as received, with no further treatment to retain their original electronic and structural properties. Our recent work has shown that acidified THF containing 5% trifluoroacetic acid (TFA) is a good solvent medium to form and solubilize conjugated $Zn^{II}$–por-

  

phyrin polymer–SWNT nanocomposites.[15] The same solvent system was again found to be ideal in the present work, especially since the triply fused $Zn^{II}$–porphyrin oligomers are highly stable towards TFA in THF (unlike the monomer), with no observable demetalation. This is likely due to a stabilizing effect of extended conjugation in these structures, and is indicated by a lack of any changes in the UV/Vis and $^1$H NMR spectra of the oligomers upon addition of TFA. It should be noted that dissolving the oligomers in THF acidified with $H_2SO_4$ instead of TFA resulted in slow demetalation, as indicated by new peaks in the UV/Vis absorption spectrum (see Supporting Information).

In a typical experiment, a SWNT sample (1.0 mg) was added to a solution of porphyrin (2.0 mg) in acidified THF (5 mL) and the mixture was sonicated for 1 h. This was followed by ultra-filtration through a 450 nm-pore Teflon membrane and repeated washings with acidified THF until the filtrate was colorless, indicating the removal of all excess porphyrin. The residue was re-suspended in acidified THF (5 mL) with sonication for 5 min. When this procedure was carried out with monomer **1**, re-suspension of the SWNT residue resulted in no observable nanotube solubility, indicating that the porphyrin monomer was completely removed by our washing procedure, and no significant interaction between **1** and the SWNTs exists. In contrast, when the above procedure was performed with a solution of the triply fused dimer in acidified THF, sonication of the isolated residue resulted in the initial formation of a homogeneous solution, which was stable enough for characterization by UV/Vis/NIR absorption spectroscopy. However, upon standing for several hours, the SWNTs were observed to precipitate, indicating that the solubilizing influence of the triply fused dimer **2** could not overcome the inter-nanotube van der Waals attraction that causes SWNTs to aggregate into bundles. When trimer **3** was used, a very stable, dark solution was obtained after sonication of the isolated residue for 5 min. This solution remained stable upon standing indefinitely, with no sedimentation even after centrifugation for 20 min at 5000 rpm (see Figure 4). This stability indicates that the interaction between trimer **3** and the nanotube sidewall must be extremely strong, preventing nanotube re-bundling after formation of the nanotube–trimer complex.

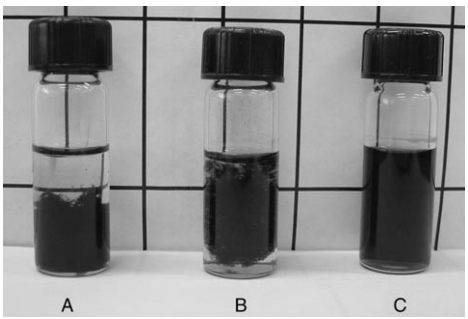


Figure 4. Photograph of three samples in acidified THF (containing 5% TFA). SWNT complexes of A) monomeric **1**, B) dimeric **2**, and C) trimeric **3**.

Clearly, the triply fused trimeric porphyrin exhibits stronger binding interactions than the monomeric and dimeric systems due to extended π conjugation and enhanced electron-donating character. Interestingly, when the above experiments were performed with pure THF as the solvent, nanotube solubility was not observed to any extent when each of the three porphyrin compounds was tested. In further control experiments, addition of acetic acid or potassium trifluoroacetate also did not result in any solubilization of the SWNTs. This indicates that addition of TFA is critical to the supramolecular interaction of the porphyrin oligomers with nanotubes in THF. The exact reason for this effect is unclear and is the subject of further investigation.

The supramolecular interaction of the triply fused dimeric and trimeric porphyrins with SWNTs was further investigated by UV/Vis and NIR absorption spectroscopy. Figure 5

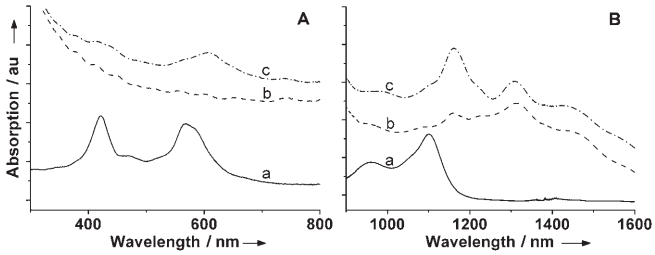


Figure 5. A) UV/Vis and B) NIR absorption spectra of a) **2** in acidified THF, b) pristine SWNTs in DMF, and c) **2**–SWNTs in acidified THF.

depicts the spectra of dimeric **2** and its SWNT complex in acidified THF. Upon complexation to SWNTs, a bathochromic shift of both the Soret and the Q-bands relative to the dimer alone was observed. The longer wavelength component of the split Soret band was observed to shift from 567 to 608 nm, while the Q-band shifted from 1100 to 1161 nm. Figure 6 illustrates similar data for trimeric **3** and its complex in acidified THF. Here, a larger bathochromic shift was observed for both the Soret bands and Q-bands relative to **3** alone, with the longer-wavelength component of the Soret band shifting from 680 to 714 nm, and the Q-band shifting from 1430 to 1530 nm. These shifts in the absorption spectra upon oligoporphyrin complexation to SWNTs are a clear manifestation of electronic interactions between the porphyrins and the nanotubes, possibly signifying a porphyrin-

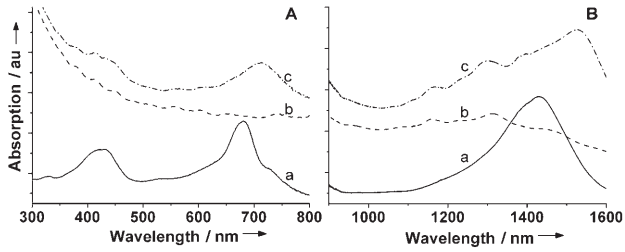


Figure 6. A) UV/Vis and B) NIR absorption spectra of a) **3** in acidified THF, b) pristine SWNTs in DMF, c) and **3**–SWNTs in acidified THF.

  

to-nanotube charge transfer. However, the specific nature of this electronic interaction is yet unknown and remains under investigation. Most significantly, with the triply fused oligomers, we detected very little, if any, absorption of the free dimer and trimer in equilibrium with the nanotube-bound oligoporphyrins. This indicates that the triply fused oligoporphyrins form very strong, and in the case of **3**, nearly irreversible complexes with SWNTs, unlike all previous reports of nanotube–porphyrin interactions.

The **3**–SWNT complex was further investigated by atomic force microscopy (AFM; Figure 7). The AFM image of this material was acquired by spin-coating (2500 rpm) three

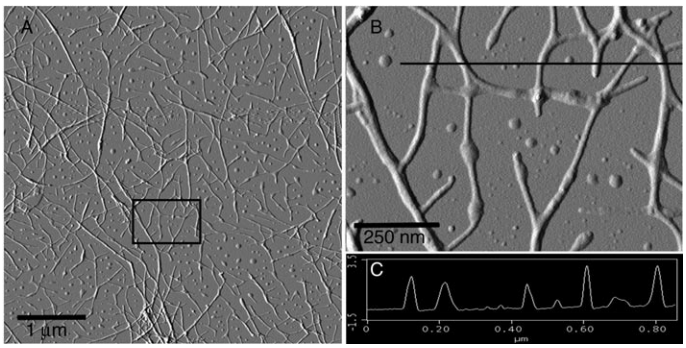


Figure 7. AFM images of the **3**–SWNT complex spin coated onto mica. A) 5×5 µm image, with a black box showing the region magnified in B). The height profile along the horizontal line of B) is shown in C).

drops of the nanotube–trimer solution in acidified THF onto freshly cleaved mica. From this experiment, the features observed on the mica surface are consistent with the existence of an interlinked network of porphyrin-coated SWNTs. Surprisingly, the height profile of most features shown is consistently in the 2–4 nm range, indicating that large nanotube bundles must have been exfoliated into either individual nanotubes or very small bundles that are coated with porphyrin trimer molecules. In addition, upon magnification of various regions in the sample (Figure 7B), it was found that the porphyrin coating on the nanotubes is relatively uniform, with practically no observable uncoated SWNTs. This again demonstrates that the SWNT–trimer interaction is exceptionally strong, allowing for complete coverage of the nanotube surface.

## Conclusions

We have shown that triply fused $Zn^{II}$–oligoporphyrin molecules exhibit interesting photophysical and electrochemical properties. These highly conjugated structures display significant bathochromic shifts in their absorption spectra relative to their monomeric and *meso–meso*-linked oligomeric counterparts. CV and DPV reveal that the electrochemical behavior is increasingly different going from monomeric porphyrin **1**, to dimeric **2**, and to trimeric **3**. Splitting of the redox waves is observed for triply fused porphyrin dimer **2** and trimer **3** owing to electron delocalization. The electrochemical HOMO–LUMO gap in monomer **1** is much larger than those of dimer **2** and trimer **3**, a direct consequence of the electronic delocalization over all porphyrin rings in the triply fused arrays. The larger peak-to-peak separation of the first two reductions and oxidations observed for trimer **3** in THF, compared with the same ones in $CH_2Cl_2$, could probably be ascribed to the coordination of the furan oxygen to the $Zn^{II}$ centers. These properties give rise to a high degree of complementarity between the oligoporphyrins and SWNTs (known to act as good electron acceptors) allowing for the occurrence of strong supramolecular interactions that are directly proportional to oligoporphyrin length. The trimeric porphyrin **3** imparted a high degree of SWNT solubility as a result of nearly irreversible complex formation, with no observable precipitation of the nanotubes over time. This was corroborated by absorption spectroscopy, for which bathochromic shifts of the oligoporphyrin bands were observed upon mixing with SWNTs. Additionally, AFM measurements indicated that oligoporphyrin adsorption can result in the exfoliation of large nanotube bundles into either individual SWNTs, or small nanotube bundles that are uniformly coated with the oligoporphyrins.

## Experimental Section

**General**: Chemicals were purchased from Aldrich, Acros, Lancaster, and Fluka and were used as received. THF was freshly distilled from sodium and benzophenone, toluene from sodium, $CH_2Cl_2$ from $CaH_2$. Moisture or air sensitive reactions were performed under an inert atmosphere of Ar by applying a positive pressure. Flash chromatography was carried out with silica gel 60 (particle size 0.04–0.063 mm, 230–400 mesh) from Fluka or with ICN alumina B (neutral, activity grade III) and distilled technical-grade solvents. Preparative size-exclusion chromatography was performed by using a glass-column (4.5×180 cm) filled with Bio-Rad Bio-Beads S-X3 and elution with $CH_2Cl_2$ at RT; flow rate approximately 40 drops (~0.84 mL min$^{-1}$) operated with gravity. The styrene–divinylbenzene copolymer gel was allowed to swell for 24 h prior to use. IR spectra were recorded on a Perkin–Elmer FT16000 spectrometer. The samples were prepared as KBr pellets, as solutions in $CHCl_3$, or as neat compounds. Selected bands are reported by wavenumber (cm$^{-1}$), and their relative intensities are described as s (strong), m (medium), or w (weak). UV/Vis/NIR spectra were recorded on a Varian-CARY 5 spectrophotometer. All spectra were measured as solutions in the indicated solvents at room temperature (RT) using a 1 cm cell. Absorption maxima ($\lambda_{max}$) are reported in nm and extinction coefficients ($\varepsilon$) in dm$^{-3}$mol$^{-1}$cm$^{-1}$. NMR spectra were recorded on a Varian Gemini 300 spectrometer. The chemical shifts ($\delta$) are given in ppm with respect to the residual non-deuterated solvent. Coupling constants ($J$) are given in Hz. All $^{13}$C NMR spectra were proton wide-band decoupled. HR-MALDI-TOF mass spectra were recorded using and an Ion Spec Ultima FT-ICR instrument. 3-Hydroxylpicolinic acid (3-HPA) or 2-[(2*E*)-3-(4-*tert*-butylphenyl)-2-methylprop-2-enylidene] malononitrile (DCTB) were used as matrices for the MALDI experiments. Melting points were determined using a Büchi Smp 20 apparatus. All melting points were measured in open capillaries and reported uncorrected. Electrochemical measurements for the target compound were performed with the CHI 660 Electrochemical Workstation. 0.1 M $n$Bu$_4$NPF$_6$ in $CH_2Cl_2$ or THF was used as the supporting electrolyte (degassed with Ar). A platinum wire was employed as the counter electrode and an Ag wire used as the pseudo-reference electrode. Ferrocene (Fc) was added as an internal reference, and the potentials were measured rel-

  

ative to the $Fc/Fc^+$ couple. A glassy carbon electrode (CHI, 1.5 mm in diameter), polished with aluminum paste and ultrasonicated in deionized water and $CH_2Cl_2$ bath, was used as the working electrode. Experiments were performed at room temperature. Ultrasonication was done in a Branson Ultrasonics B1510 bath sonicator. Atomic force microscopy (AFM) was performed using a Digital Instruments NanoScope IIIa Multimode AFM, with samples prepared by spin coating (2500 rpm) onto freshly cleaved mica substrates. The images were recorded with standard tips in tapping mode at a scan rate of 1.0 Hz.

**[5,15-Bis(3,5-di-*tert*-butylphenyl)-10,20-dibromoporphyrinato(2−)-κ*N*$^{21}$, κ*N*$^{22}$,κ*N*$^{23}$,κ*N*$^{24}$]zinc(II) (5)**: NBS (154 mg, 0.94 mmol) was added to a stirred solution of porphyrin **4** (350 mg, 0.47 mmol) in $CH_2Cl_2$ (50 mL) and pyridine (1.5 mL) at 0 °C under Ar. After 10 min, the reaction was quenched with acetone (5 mL) and the solvent was removed. The residue was washed with MeOH (3×10 mL) and the resulting solid dried to give the title compound as purple crystals (391 mg, 90 %). M.p. > 300 °C; $^1$H NMR ([D$_8$]THF, 300 MHz): $\delta$ = 1.57 (s, 36H), 7.91 (t, $J$ = 1.5 Hz, 2H), 8.06 (d, $J$ = 1.8 Hz, 4H), 8.88 (d, $J$ = 4.5 Hz, 4H), 9.66 ppm (d, $J$ = 4.8 Hz, 4H); $^{13}$C NMR ([D$_8$]THF, 75 MHz): $\delta$ = 33.42, 37,16, 106.44, 123.42, 125.63, 132.27, 134.85, 135.67, 144.23, 150.91, 152.34, 153.41 ppm; IR (neat): $\tilde{\nu}$ = 2959 (m), 2863 (w), 1797 (w), 1590 (m), 1514 (w), 1497 (w), 1474 (m), 1423 (w), 1391 (w), 1360 (m), 1320 (m), 1285 (m), 1245 (m) 1200 (w), 1070 (m), 1021 (w), 1000 (s), 929 (w), 898 (m), 882 (m), 815 (m), 788 (s), 725 (m), 713 (m), 695 (s), 617 cm$^{-1}$ (w); UV/Vis ($CHCl_3$): $\lambda_{max}$ ($\varepsilon$) = 427 (198100), 565 nm (6840 dm$^3$mol$^{-1}$cm$^{-1}$); HR-MALDI-MS (3-HPA): $m/z$ calcd for $C_{48}H_{50}Br_2N_4Zn$ $[M]^+$: 904.1694; found: 904.1700.

**[5,15-Bis(4-cyanophenyl)-10,20-bis(3,5-di-*tert*-butylphenyl)porphyrinato(2−)-κ*N*$^{21}$,κ*N*$^{22}$,κ*N*$^{23}$,κ*N*$^{24}$]zinc(II) (1)**: A 250 mL round-bottomed flask was charged with porphyrin **5** (785 mg, 0.86 mmol) in toluene (150 mL), and **6** (820 mg, 3.84 mmol), [Pd(PPh$_3$)$_4$] (100 mg, 0.086 mmol), and $Cs_2CO_3$ (4.0 g, 12.3 mmol) were added. The mixture was degassed by bubbling Ar through for 30 min, then heated to reflux under Ar for 18 h. The mixture was filtered through a pad of Celite and the solvent evaporated in vacuo. Flash chromatography ($SiO_2$, hexane/$CH_2Cl_2$, 1:2) afforded the desired product as a purple solid (830 mg, 97 %). M.p. > 300 °C; $^1$H NMR ($CDCl_3$, 300 MHz): $\delta$ = 1.61 (s, 36H), 7.89 (t, $J$ = 1.5 Hz, 2H), 8.04 (d, $J$ = 7.8 Hz, 2H), 8.16 (d, $J$ = 1.2 Hz, 4H), 8.40 (d, $J$ = 7.8 Hz, 4H), 8.90 (d, $J$ = 4.5 Hz, 4H), 9.12 ppm (d, $J$ = 4.5 Hz, 4H); $^{13}$C NMR ($CDCl_3$, 75 MHz): $\delta$ = 31.93, 35.23, 111.53, 118.67, 118.97, 121.11, 123.34, 127.76, 129.85, 130.31, 131.28, 132.73, 133.08, 134.80, 141.35, 147.89, 148.70, 149.21, 150.73 ppm; IR (neat): $\tilde{\nu}$ = 2950 (m), 2865 (w), 227 (m), 1805 (w), 1591 (m), 1523 (m), 1475 (m), 1423 (w), 1392 (m), 1361 (m), 1290 (w), 1246 (m), 1220 (m), 1202 (m), 1176 (w), 1073 (m), 1000 (s), 934 (m), 898 (m), 874 (m), 820 (m), 794 (m), 772 (s), 713 (s), 671 cm$^{-1}$ (w); UV/Vis ($CHCl_3$): $\lambda_{max}$ ($\varepsilon$) = 427 (201200), 556 nm (7600 dm$^3$mol$^{-1}$cm$^{-1}$); HR-MALDI-MS (DCTB): $m/z$ calcd for $C_{62}H_{58}N_6Zn$ $[M]^+$: 950.4009; found: 950.3998.

**[10,20-Bis(3,5-di-*tert*-butylphenyl)5-bromoporphyrinato(2−)-κ*N*$^{21}$,κ*N*$^{22}$, κ*N*$^{23}$,κ*N*$^{24}$]zinc(II) (7)**: NBS (150 mg, 0.84 mmol) was added to a stirred solution of porphyrin **4** (626 mg, 0.84 mmol) in $CH_2Cl_2$ (65 mL) and pyridine (1.0 mL) at 0 °C under Ar. After 10 min, the reaction was quenched with acetone (10 mL) and the solvent removed in vacuo. The residue was washed with MeOH (3×10 mL), and the resulting solid was dried to give a mixture of monobromoporphyrin **7** (major) and small amounts of dibromoporphyrin **5** and porphyrin **4**. Isolation of pure **7** by flash chromatography was difficult due to the very close polarity of the three compounds, and therefore **7** was directly used for the next step reaction without isolation and characterization.

**[10,20-Bis(3,5-di-*tert*-butylphenyl)-5-(4-Cyanophenyl)porphyrinato(2−)-κ*N*$^{21}$,κ*N*$^{22}$,κ*N*$^{23}$,κ*N*$^{24}$]zinc(II) (8)**: The crude monobromoporphyrin **7** was placed into a 250 mL round-bottomed flask and dissolved in toluene (200 mL). Compound **6** (525 mg, 2.29 mmol), [Pd(PPh$_3$)$_4$] (105 mg, 0.09 mmol), and $Cs_2CO_3$ (2.03 g, 11.5 mmol) were added to this solution. The mixture was degassed by bubbling Ar through for 30 min, then heated to reflux under Ar for 18 h. The mixture was filtered through a pad of Celite and the solvent evaporated in vacuo. The product was then purified by flash chromatography ($SiO_2$, hexane/$CH_2Cl_2$, 1:1) allowing its isolation as a red solid (500 mg, 70 %). M.p. > 300 °C; $^1$H NMR ($CDCl_3$, 300 MHz): $\delta$ = 1.65 (s, 36H), 7.94 (t, $J$ = 1.5 Hz, 2H), 8.05 (d, $J$ = 8.1 Hz, 2H), 8.22 (d, $J$ = 1.5 Hz, 4H), 8.41 (d, $J$ = 8.1 Hz, 2H), 8.94 (d, $J$ = 4.2 Hz, 2H), 9.19 (d, $J$ = 4.2 Hz, 2H), 9.26 (d, $J$ = 4.8 Hz, 2H), 9.47 (d, $J$ = 4.8 Hz, 2H), 10.32 ppm (s, 1H); $^{13}$C NMR ($CDCl_3$, 75 MHz): $\delta$ = 31.98, 35.28, 106.46, 111.40, 118.36, 119.10, 121.01, 122.45, 129.92, 130.24, 130.99, 131.94, 132.77, 133.15, 134.81, 141.43, 148.22, 148.68, 148.72, 149.91, 150.43, 150.73 ppm; IR (neat): $\tilde{\nu}$ = 2953 (m), 2868 (w), 225 (w), 1712 (w), 1589 (m), 1522 (w), 1475 (w), 1391 (w), 1360 (m), 1325 (w), 1290 (m), 1218 (m), 1207 (m), 1174 (w), 1065 (m), 1042 (w), 1000 (s), 926 (m), 899 (m), 885 (m), 857 (m), 78 (m), 791 (s), 706 (s), 659 cm$^{-1}$ (w); UV/Vis ($CHCl_3$): $\lambda_{max}$ ($\varepsilon$) = 421 (186500), 549 nm (7300 dm$^3$mol$^{-1}$cm$^{-1}$); HR-MALDI-MS (DCTB): $m/z$ calcd for $C_{55}H_{55}N_5Zn$ $[M]^+$: 849.3743; found: 849.3733.

**{μ-[10,10′-Bis(4-cyanophenyl)-5,5′,15,15′-tetrakis(3,5-di-*tert*-butylphenyl)-18,18′:20,20′-dicyclo-2,2′-biporphyrinato(4−)-κ*N*$^{21}$,κ*N*$^{22}$,κ*N*$^{23}$,κ*N*$^{24}$:κ*N*$^{21'}$, κ*N*$^{22'}$,κ*N*$^{23'}$,κ*N*$^{24'}$]}dizinc(II) (2)**: Porphyrin **8** (150 mg, 0.18 mmol), DDQ (201 mg, 0.9 mmol), and Sc(OTf)$_3$ (435 mg, 0.9 mmol) were dissolved in toluene (100 mL) , and the mixture was heated to reflux under Ar for 2 h. THF (30 mL) was added, and the solution was stirred for a further 1 h at room temperature. The mixture was passed over a column of alumina, and the solvent was removed in vacuo, affording a black powder (105 mg, 70 %). M.p. > 300 °C; $^1$H NMR ($CDCl_3$, 300 MHz): $\delta$ = 1.47 (s, 36H), 7.34 (s, 4H), 7.57 (d, $J$ = 4.8 Hz, 4H), 7.64 (m, 12H), 7.72 (d, $J$ = 4.8 Hz, 4H), 7.87 (d, $J$ = 8.4 Hz, 4H), 7.93 ppm (d, $J$ = 8.4 Hz, 4H); $^{13}$C NMR ($CDCl_3$, 75 MHz): $\delta$ = 31.80, 35.05, 111.37, 118.93, 126.51, 127.55,33.32, 135.93, 139.82, 146.55, 148.75, 151.67, 153.44, 153.81, 154.18 ppm; IR (neat): $\tilde{\nu}$ = 2961 (m), 2238 (w), 1593 (m), 1476 (s), 1393 (w), 1363 (m), 1345 (w), 1300 (m), 1266 (w), 1247 (m), 1225 (w), 1199 (s), 1074 (w), 1023 (m), 1001 (m), 943 (s), 900 (m), 881 (m), 826 (m), 791 (s), 724 (m), 716 (m), 696 (m), 658 (w); UV/Vis ($CHCl_3$): $\lambda_{max}$ ($\varepsilon$) = 422 (163100), 464 (59400), 565 (146400), 955 (20500), 1087 nm (33400 dm$^3$mol$^{-1}$cm$^{-1}$); HR-MALDI-MS (DCTB): $m/z$ calcd for $C_{110}H_{104}N_{10}Zn_2$ $[M]^+$: 1692.7023; found: 1692.7006.

**[5,15-Bis(3,5-di-*tert*-butylphenyl)-10-bromo-20-(4-cyanophenyl)porphyrinato(2−)-κ*N*$^{21}$,κ*N*$^{22}$,κ*N*$^{23}$,κ*N*$^{24}$]zinc(II) (9)**: NBS (108 mg, 0.61 mmol) was added to a stirred solution of porphyrin **8** (518 mg, 0.61 mmol) in $CH_2Cl_2$ (100 mL) and pyridine (2.0 mL) at 0 °C under Ar. After 10 min, the reaction was quenched with acetone (10 mL) and the solvent was evaporated in vacuo. The residue was purified by flash chromatography ($SiO_2$, $CH_2Cl_2$/hexane, 1:1) affording the product as a purple solid (488 mg, 86 %). M.p. > 300 °C; $^1$H NMR ($CDCl_3$, 300 MHz): $\delta$ = 1.58 (s, 36H), 7.83 (t, $J$ = 1.5 Hz, 2H), 8.02 (d, $J$ = 8.1 Hz, 2H), 8.06 (d, $J$ = 2.1 Hz, 4H), 8.33 (d, $J$ = 8.1 Hz, 2H), 8.78 (d, $J$ = 4.5 Hz, 2H), 8.97 (d, $J$ = 4.5 Hz, 2H), 9.05 (d, $J$ = 4.5 Hz, 2H), 9.78 ppm (d, $J$ = 4.5 Hz, 2H); $^{13}$C NMR ($CDCl_3$, 75 MHz): $\delta$ = 32.00, 35.18, 105.75, 111.96, 118.91, 121.42, 123.73, 130.12, 130.55, 131.55, 133.41, 133.52, 133.95, 135.04, 141.48, 147.96, 148.88, 149.76, 150.05, 151.02, 151.48 ppm; IR (neat): $\tilde{\nu}$ = 2951 (m), 2865 (w), 229 (m), 1590 (m), 1518 (w), 1496 (w), 1425 (w), 1391 (w), 1361 (m), 1323 (m), 1289 (w), 1241 (m), 1206 (w), 1145 (w), 1070 (m), 1000 (s), 934 (m), 898 (w), 860 (w), 817 (s), 787 (m), 733 (w), 724 (m), 714 (s), 652 cm$^{-1}$ (w); UV/Vis ($CHCl_3$): $\lambda_{max}$ ($\varepsilon$) = 428 (199200), 560 nm (7430 dm$^3$mol$^{-1}$cm$^{-1}$); HR-MALDI-MS (DCTB): $m/z$ calcd for $C_{55}H_{54}BrN_5Zn$ $[M]^+$: 927.2854; found: 927.2832.

**5,15-Bis(3,5-di-*tert*-butylphenyl)-10-(4-cyanophenyl)-20-(4,45,5-tetramethyl-[1,3,2]dioxaborolan-2-yl)porphyrinato(2−)-κ*N*$^{21}$,κ*N*$^{22}$,κ*N*$^{23}$,κ*N*$^{24}$]zinc(II) (10)**: A 250 mL two-necked flask was charged with porphyrin **9** (427 mg, 0.46 mol), $Et_3N$ (5.0 mL, 39.60 mmol), and 1,2-dichloroethane (100 mL). The mixture was degassed by bubbling with Ar for 30 min, after which pinacolborane (3.0 mL, 18.90 mmol) and [$PdCl_2(PPh_3)_2$] (35 mg, 0.05 mmol) were added. The resulting solution was heated to reflux for 1.5 h and quenched with water (10 mL), followed by washing with water (3× 50 mL). The organic phase was dried over $Na_2SO_4$, and the solvent was removed. The residue was purified by flash chromatography ($SiO_2$, $CH_2Cl_2$/hexane, 3:1) to give the desired product as a red solid (377 mg, 84 %). M.p. > 300 °C; $^1$H NMR ($CDCl_3$, 300 MHz): $\delta$ = 1.62 (s, 36H), 1.91 (s, 12H), 7.89 (t, $J$ = 1.8 Hz, 2H), 8.05 (d, $J$ = 8.4 Hz, 2H), 8.16 (d, $J$ = 1.5 Hz, 4H), 8.38 (d, $J$ = 8.1 Hz, 2H), 8.89 (d, $J$ = 4.8 Hz, 2H), 9.10 (d, $J$ = 4.8 Hz, 2H), 9.20 (d, $J$ = 4.5 Hz, 2H), 9.98 ppm (d, $J$ = 4.8 Hz, 2H);

  

$^{13}$C NMR ($CDCl_3$, 75 MHz): $\delta$ = 25.64, 32.07, 35.36, 85.57, 110.67, 121.17, 122.90, 128.52, 129.06, 129.59, 130.07, 130.53, 131.16, 131.36, 132.63, 133.19, 133.77, 142.00, 148.50, 148.88, 150.85, 150.94, 154.64 ppm; IR (neat): $\tilde{\nu}$ = 2959 (m), 225 (w), 1725 (w), 1590 (m), 1525 (m), 1448 (w), 1391 (w), 1360 (m), 1305 (w), 1277 (m), 1201 (m), 1140 (s), 1069 (m), 1035 (m), 1000 (s), 964 (w), 928 (m), 875 (w), 852 (m), 817 (m), 791 (s), 766 (w), 715 (s), 658 cm$^{-1}$ (m); UV/Vis ($CHCl_3$): $\lambda_{max}$ ($\varepsilon$) = 424 (186 600), 552 nm (6500 dm$^3$ mol$^{-1}$ cm$^{-1}$); HR-MALDI-MS (DCTB): *m*/*z* calcd for $C_{61}H_{66}BN_5O_2Zn$ $[M]^+$: 975.4601; found: 975.4596.

**Preparation of 11 via Pd-catalyzed cross coupling between 5 and 10**: Porphyrins **5** (35 mg, 0.0386 mmol) and **10** (76 mg, 0.0772 mmol), $Cs_2CO_3$ (100 mg), and $[Pd(PPh_3)_4]$ (10 mg, 0.0086 mmol) were dissolved in a mixture of dry DMF (5 mL) and dry toluene (5 mL). The solution was deoxygenated by means of four freeze-pump-thaw cycles, and the resulting mixture was heated at 90 °C overnight under Ar. The mixture was extracted with $CH_2Cl_2$ (50 mL) and washed with water (3 × 30 mL). The organic layer was dried over $Na_2SO_4$ and concentrated. The components in the resulting residue were separated by flash chromatography ($SiO_2$, $CH_2Cl_2$/hexane, 3:1), resulting in four fractions. The first three fractions corresponded to porphyrin monomer **4** (9.0 mg, 35 %), dimer **12** (22 mg, 18 %), and monomer **8** (17.2 mg, 26 %). The fourth fraction was a mixture of the homocoupling product, dimer **13**, and the target cross-coupling product, trimer **11**. This mixture was separated by preparative size-exclusion chromatography on Bio-Rad Bio-Beads S-X3 to give the final pure products **13** (15 mg, 24 %) and **11** (16 mg, 17 %) as brown solids.

**Data for {μ-[15-(4-Cyanophenyl)-10,10′,20,20′-tetrakis(3,5-di-*tert*-butylphenyl)-5,5′-biporphyrinato(4−)-κ*N*$^{21}$,κ*N*$^{22}$,κ*N*$^{23}$,κ*N*$^{24}$:κ*N*$^{21'}$,κ*N*$^{22'}$,κ*N*$^{23'}$,κ*N*$^{24'}$]}dizinc(II) (12)**: M.p. > 300 °C; $^1$H NMR ($CDCl_3$, 300 MHz): $\delta$ = 1.53 (s, 36H), 1.55 (s, 36H), 7.79 (t, *J* = 1.8 Hz, 2H), 7.81 (t, *J* = 1.8 Hz, 2H), 8.18 (d, *J* = 1.8 Hz, 4H), 8.21 (d, *J* = 1.8 Hz, 4H), 8.25 (d, *J* = 5.1 Hz, 2H), 8.26 (d, *J* = 5.1 Hz, 2H), 8.53 (d, *J* = 8.1 Hz, 2H), 8.87 (d, *J* = 4.8 Hz, 2H), 9.00 (d, *J* = 4.5 Hz, 2H), 9.16 (d, *J* = 4.5 Hz, 2H), 9.29 (d, *J* = 4.8 Hz, 2H), 9.58 (d, *J* = 4.5 Hz, 2H), 10.48 ppm (s, 1H); $^{13}$C NMR ($CDCl_3$, 75 MHz): $\delta$ = 31.93, 31.97, 35.25, 35.26 106.87, 111.78, 118.92, 119.77, 120.65, 121.10, 121.18, 123.23, 124.02, 129.93, 129.99, 130.65, 131.32, 132.07, 132.52, 132.71, 132.98, 133.12, 134.12, 134.48, 135.15, 141.71, 141.79, 148.51, 148.86, 149.28, 150.07, 150.28, 150.68, 151.26, 151.30, 154.73, 155.27 ppm; IR (neat): $\tilde{\nu}$ = 2959 (m), 226 (w), 1803 (w), 1590 (m), 1520 (w), 1475 (w), 1423 (w), 1391 (w), 1382 (w), 1318 (w), 1289 (m), 1246 (m), 1220 (w), 1208 (w), 1063 (m), 1000 (s), 927 (m), 898 (m), 881 (w), 863 (w), 846 (w), 821 (m), 791 (m), 713 (s), 615 cm$^{-1}$ (w); UV/Vis ($CHCl_3$): $\lambda_{max}$ ($\varepsilon$) = 421 (220 900), 456 (209 600), 563 nm (9600 dm$^3$ mol$^{-1}$ cm$^{-1}$); HR-MALDI-MS (DCTB): *m*/*z* calcd for $C_{103}H_{105}N_9Zn_2$ $[M]^+$: 1595.7076; found: 1595.7061.

**Data for {μ-[15,15′-Bis(4-Cyanophenyl)-10,10′,20,20′-tetrakis(3,5-di-*tert*-butylphenyl)-5,5′-biporphyrinato(4−)-κ*N*$^{21}$,κ*N*$^{22}$,κ*N*$^{23}$,κ*N*$^{24}$:κ*N*$^{21'}$,κ*N*$^{22'}$,κ*N*$^{23'}$,κ*N*$^{24'}$]}dizinc(II) (13)**: M.p. > 300 °C; $^1$H NMR ($CDCl_3$, 300 MHz): $\delta$ = 1.46 (s, 72H), 7.72 (t, *J* = 1.5 Hz, 4H), 8.09 (d, *J* = 1.5 Hz, 8H), 8.12 (d, *J* = 7.5 Hz, 4H), 8.15 (d, *J* = 4.8 Hz, 4H), 8.46 (d, *J* = 7.5 Hz, 4H), 8.74 (d, *J* = 4.5 Hz, 4H), 8.92 (d, *J* = 5.1 Hz, 4H), 9.08 ppm (d, *J* = 5.1 Hz, 4H); $^{13}$C NMR ($CDCl_3$, 75 MHz): $\delta$ = 31.86, 35.17, 11.57, 118.76, 119.515, 119.96, 120.96, 123.80, 129.67, 130.39, 131.12, 132.51, 132.77, 134.10, 134.88, 141.41, 148.17, 148.58, 149.04, 150.35, 150.99, 154.86 ppm; IR (neat): $\tilde{\nu}$ = 2951 (m), 226 (w), 1804 (w), 1589 (m), 1519 (m), 1422 (w), 1391 (m), 1361 (m), 1330 (w), 1285 (m), 1246 (m), 1205 (m), 1067 (m), 1000 (s), 928 (s), 898 (m), 876 (w), 822 (m), 810 (w), 792 (m), 712 (s), 616 cm$^{-1}$ (m); UV/Vis ($CHCl_3$): $\lambda_{max}$ ($\varepsilon$) = 421 (245 600), 456 (237 000), 563 nm (53 400 dm$^3$ mol$^{-1}$ cm$^{-1}$); HR-MALDI-MS (3-HPA): *m*/*z* calcd for $C_{110}H_{108}N_{10}Zn_2$ $[M]^+$: 1696.7341; found: 1696.7272.

**Data for {μ$_3$-[15,15″-Bis(4-cyanophenyl)-10,10′10″,20,20′20″-hexakis(3,5-di-*tert*-butylphenyl)-5,5′:15′,5″-terporphyrinato(6−)-κ*N*$^{21}$,κ*N*$^{22}$,κ*N*$^{23}$,κ*N*$^{24}$:κ*N*$^{21'}$,κ*N*$^{22'}$,κ*N*$^{23'}$,κ*N*$^{24'}$:κ*N*$^{21''}$,κ*N*$^{22''}$,κ*N*$^{23''}$,κ*N*$^{24''}$]}trizinc(II) (11)**: M.p. > 300 °C; $^1$H NMR ($CDCl_3$, 300 MHz): $\delta$ = 1.38 (s, 36H), 1.50 (s, 72H), 7.61 (t, *J* = 1.8 Hz, 2H), 7.59 (t, *J* = 1.8 Hz, 4H), 8.10 (d, *J* = 1.8 Hz, 4H), 8.14 (d, *J* = 1.8 Hz, 8H), 8.14 (d, *J* = 7.5 Hz, 4H), 8.21 (d, *J* = 4.8 Hz, 4H), 8.30 (d, *J* = 4.5 Hz, 4H), 8.49 (d, *J* = 7.5 Hz, 4H), 8.76 (d, *J* = 4.5 Hz, 4H), 8.81 (d, *J* = 4.8 Hz, 4H), 8.94 (d, *J* = 4.8 Hz, 4H), 9.10 ppm (d, *J* = 4.5 Hz, 4H); $^{13}$C NMR ($CDCl_3$/$CS_2$, 75 MHz): $\delta$ = 31.82, 31.91, 34.94, 35.06, 111.69, 118.67, 118.84, 119.95, 120.30, 120.94, 123.74, 124.14, 129.50, 129.73, 130.32, 131.09, 132.16, 132.24, 132.50, 132.82, 134.05, 134.32, 135.00, 141.56, 148.11, 148.25, 148.43, 148.98, 150.38, 150.46, 150.94, 154.63, 154.84 ppm; IR (neat): $\tilde{\nu}$ = 2952 (m), 2863 (w), 2230 (w), 1590 (m), 1519 (w), 1474 (w), 1422 (w), 1391 (w), 1360 (m), 1320 (w), 1286 (m), 1246 (m), 1206 (m), 1066 (w), 1000 (s), 927 (m), 899 (w), 883 (w), 822 (m), 792 (s), 755 (w), 722 (m), 713 (s), 616 cm$^{-1}$ (w); UV/Vis ($CHCl_3$): $\lambda_{max}$ ($\varepsilon$) = 420 (292 000), 479 (260 700), 571 nm (83 000 dm$^3$ mol$^{-1}$ cm$^{-1}$); HR-MALDI-MS (DCTB): *m*/*z* calcd for $C_{158}H_{158}N_{14}Zn_3$ $[M]^+$: 2443.0663; found: 2443.0600.

**{μ$_3$-[10,10″-Bis(4-cyanophenyl)-5,5′5″,15,15′15″-hexakis(3,5-di-*tert*-butylphenyl)-18,18′:20,20′:10′,20″:12′,18″-tetracyclo-2,2′:8′2″-terporphyrinato(6−)-κ*N*$^{21}$,κ*N*$^{22}$,κ*N*$^{23}$,κ*N*$^{24}$:κ*N*$^{21'}$,κ*N*$^{22'}$,κ*N*$^{23'}$,κ*N*$^{24'}$:κ*N*$^{21''}$,κ*N*$^{22''}$,κ*N*$^{23''}$,κ*N*$^{24''}$]}trizinc(II) (3)**: Porphyrin **11** (60 mg, 0.024 mmol), DDQ (60 mg, 0.24 mmol), and $Sc(OTf)_3$ (125 mg, 0.24 mmol) were dissolved in dry toluene (30 mL) , and the mixture was heated to reflux under Ar for 2 h. The mixture was passed over an alumina column, eluting first with $CH_2Cl_2$ and then with $CH_2Cl_2$/THF (5:1), resulting in the collection of a green fraction. The solvent was removed in vacuo, and the residue was purified by flash chromatography ($SiO_2$, $CH_2Cl_2$/hexane, 1:1), affording the product as a black powder (60 mg, quant.). M.p. > 300 °C; $^1$H NMR ($CDCl_3$/$CS_2$, 300 MHz): $\delta$ = 1.31 (s, 36H), 1.34 (s, 72H), 6.86 (s, 4H), 6.89 (s, 4H), 7.39 (m, 6H), 7.52 (d, *J* = 4.5, 4H), 7.60 (m, 12H), 7.72 (d, *J* = 4.5, 4H), 7.87 (d, *J* = 8.4, 4H), 7.93 ppm (d, *J* = 8.4, 4H); IR (neat): $\tilde{\nu}$ = 3625 (w), 2949 (m), 2359 (w), 2226 (m), 1715 (w), 1698 (w), 1694 (w), 1651 (w), 1589 (m), 1475 (w), 1391 (m), 1360 (m), 1299 (m), 1245 (m), 1224 (m), 1000 (s), 1117 (m), 1002 (s), 940 (m), 898 (m), 876 (m), 860 (m), 823 (s), 790 (m), 767 (m), 714 (s), 667 (m), 631 cm$^{-1}$ (w); UV/Vis ($CHCl_3$, $\varepsilon$): 427 (59,100), 669 (73 900), 1185 (13 800), 1407 nm (46 800 dm$^3$ mol$^{-1}$ cm$^{-1}$); HR-MALDI-MS (3-HPA): *m*/*z* calcd for $C_{158}H_{150}N_{14}Zn_3$ $[M]^+$: 2435.0037; found: 2435.0001.

## Acknowledgements

We gratefully acknowledge financial support from the Natural Science and Engineering Research Council of Canada (NSERC) Strategic Grants program, the Canada Foundation for Innovation (CFI), the Ontario Innovation Trust (OIT), the Materials and Manufacturing Ontario Emerging Materials Knowledge Fund (EMK), the Swiss National Science Foundation (SNF), the NCCR "Nanoscale Science", and the US National Science Foundation (NSF) CHE-0509989.

[1] A. Tsuda, A. Osuka, *Adv. Mater.* **2002**, *14*, 75–79.
[2] A. Tsuda, H. Furuta, A. Osuka, *Angew. Chem.* **2000**, *112*, 2649–2652; *Angew. Chem. Int. Ed.* **2000**, *39*, 2549–2552.
[3] A. Tsuda, A. Osuka, *Science* **2001**, *293*, 79–82.
[4] D. Bonifazi, M. Scholl, F. Y. Song, L. Echegoyen, G. Accorsi, N. Armaroli, F. Diederich, *Angew. Chem.* **2003**, *115*, 5116–5120; *Angew. Chem. Int. Ed.* **2003**, *42*, 4966–4970.
[5] D. Bonifazi, H. Spillmann, A. Kiebele, M. de Wild, P. Seiler, F. Y. Cheng, H. J. Guntherodt, T. Jung, F. Diederich, *Angew. Chem.* **2004**, *116*, 4863–4867; *Angew. Chem. Int. Ed.* **2004**, *43*, 4759–4763.
[6] R. J. Chen, Y. Zhang, D. Wang, H. Dai, *J. Am. Chem. Soc.* **2001**, *123*, 3838–3839.
[7] J. Chen, H. Y. Liu, W. A. Weimer, M. D. Halls, D. H. Waldeck, G. C. Walker, *J. Am. Chem. Soc.* **2002**, *124*, 9034–9035.
[8] H. Murakami, T. Nomura, N. Nakashima, *Chem. Phys. Lett.* **2003**, *378*, 481–485.
[9] H. P. Li, B. Zhou, Y. Lin, L. R. Gu, W. Wang, K. A. S. Fernando, S. Kumar, L. F. Allard, Y. P. Sun, *J. Am. Chem. Soc.* **2004**, *126*, 1014–1015.
[10] J. Y. Chen, C. P. Collier, *J. Phys. Chem. B* **2005**, *109*, 7605–7609.
[11] A. Satake, Y. Miyajima, Y. Kobuke, *Chem. Mater.* **2005**, *17*, 716–724.
[12] T. Hasobe, S. Fukuzumi, P. V. Kamat, *J. Am. Chem. Soc.* **2005**, *127*, 11884–11885.

  

[13] D. M. Guldi, H. Taieb, G. M. A. Rahman, N. Tagmatarchis, M. Prato, *Adv. Mater.* **2005**, *17*, 871–875.
[14] K. S. Chichak, A. Star, M. V. R. Altoe, J. F. Stoddart, *Small* **2005**, *1*, 452–461.
[15] F. Cheng, A. Adronov, *Chem. Eur. J.* DOI: 10.1002/chem.200600302.
[16] D. Bonifazi, G. Accorsi, N. Armaroli, F. Y. Song, A. Palkar, L. Echegoyen, M. Scholl, P. Seiler, B. Jaun, F. Diederich, *Helv. Chim. Acta* **2005**, *88*, 1839–1884.
[17] M. Kamo, A. Tsuda, Y. Nakamura, N. Aratani, K. Furukawa, T. Kato, A. Osuka, *Org. Lett.* **2003**, *5*, 2079–2082.
[18] D. M. Guldi, M. Marcaccio, D. Paolucci, F. Paolucci, N. Tagmatarchis, D. Tasis, E. Vazquez, M. Prato, *Angew. Chem.* **2003**, *115*, 4338–4341; *Angew. Chem. Int. Ed.* **2003**, *42*, 4206–4209.
[19] D. M. Guldi, G. N. A. Rahman, J. Ramey, M. Marcaccio, D. Paolucci, F. Paolucci, S. H. Qin, W. T. Ford, D. Balbinot, N. Jux, N. Tagmatarchis, M. Prato, *Chem. Commun.* **2004**, 2034–2035.
[20] D. M. Guldi, G. M. A. Rahman, N. Jux, N. Tagmatarchis, M. Prato, *Angew. Chem.* **2004**, *116*, 5642–5646; *Angew. Chem. Int. Ed.* **2004**, *43*, 5526–5530.
[21] G. M. A. Rahman, D. M. Guldi, R. Cagnoli, A. Mucci, L. Schenetti, L. Vaccari, M. Prato, *J. Am. Chem. Soc.* **2005**, *127*, 10051–10057.
[22] D. M. Guldi, G. M. A. Rahman, F. Zerbetto, M. Prato, *Acc. Chem. Res.* **2005**, *38*, 871–878.

Received: January 28, 2006
Published online: May 19, 2006

  